JOURNAL OF GEOPHYSICAL RESEARCH, VOL. 106, NO. C7, PAGES 13,959–13,974, JULY 15, 2001

Large-eddy simulation of the diurnal cycle of oceanic boundary layer: Sensitivity to domain size and spatial resolution

Dailin Wang

International Pacific Research Center, University of Hawaii at Manoa, Honolulu, HI

Abstract. The sensitivity of ocean large-eddy simulations (LES) to model domain size and spatial resolution is systematically investigated in the context of a diurnal cycling oceanic boundary layer. The model domain size varies by a factor of 64, horizontal resolution varies by a factor of 12, and vertical resolution varies by a factor of 8. A control experiment with a high resolution serves as the "truth" by which other experiments with smaller domains and/or coarser resolutions are judged. During nighttime the primary balance in the turbulent kinetic energy budget is between buoyancy production, turbulent transport, pressure transport, and dissipation. During daytime the primary balance is between shear production, buoyancy destruction, and dissipation. It is found that mean fields and turbulent fluxes are insensitive to domain size as long as it is comparable to or greater than the mixed layer depth. The mean fields and turbulent fluxes are also insensitive to resolution, provided there are several vertical levels in the entrainment layer. Turbulent kinetic energy (TKE), however, shows varying degrees of sensitivity. Simulations with larger domains or with coarser resolutions tend to have larger values of TKE. Furthermore, TKE is more sensitive to domain size and resolution during the day (shear turbulence) than during the night (convection). Practically, it is better to use a larger domain with an anisotropic resolution than a small domain with an isotropic resolution, if computer resources are severely limited. With the same grid geometry, the former is not only cheaper to conduct but also can be more accurate as far as turbulent kinetic energy and turbulent fluxes are concerned. This underlines the importance of resolving the largest eddies in the oceanic boundary layer. We also conclude that validations of simple one-dimensional mixed layer models using LES solutions with a resolution of order $32 \times 32 \times 32$ are not without merit in the sense that mean fields and turbulent fluxes are not much different when much higher resolution is used. However, if TKE is used as a variable of validation, higher resolution is needed.

1. Introduction

Large-eddy simulation (LES) is routinely done in the atmospheric science and the fluid mechanics communities. Its application to the study of oceanic turbulence however, is more recent. Several recent studies have shown that LES is a promising tool in studying the fundamental processes of ocean mixing [e.g., *Siegel and Domaradzki*, 1994; *Skyllingstad and Denbo*, 1995; *Denbo and Skyllingstad*, 1996; *Wang et al.*, 1996; *McWilliams et al.*, 1997; *Wang et al.*, 1998; *Skyllingstad et al.*, 1999]. The appeal of LES is that the largest eddies, which vary from flow to flow and contribute the most to turbulent fluxes, are resolved and only the subgrid scale (SGS) processes, which are more universal, are parameterized. In traditional one-dimensional (1-D) boundary layer models all processes are parameterized.

Comparison of simple 1-D mixed layer models with observations is not clean because it is difficult if not impossible to replicate the exact oceanic conditions in a 1-D model. So researchers began to use LES results to validate simple 1-D mixed layer models because comparison of 1-D models with LES is clean. For example, *Large and Gent* [1999] compared a 1-D model [*Large et al.*, 1994] with the LES results of *Wang et al.* [1998]. However, the LES results used were from numerical experiments of relatively coarse resolutions, where domain size and/or resolution were compromised in order to conduct long integrations (a few days). If LES solutions are sensitive to domain size and resolution, tuning 1-D models to coarse resolution LES results will be meaningless. These sensitivity issues need to be addressed

Paper number 2001JC000896.
0148-0227/01/2001JC000896$09.00

before ocean LES results can be used to validate simple mixed layer models.

In this study we systematically investigate the sensitivity of LES solutions to domain size and resolution. We choose the test problem to be a diurnal cycling boundary layer. During the night, turbulence is mainly driven by surface cooling, i.e., weakly sheared convection. During the day, turbulence is driven by surface wind stress, i.e., stably stratified shear turbulence. The effect of rotation is ignored. The test problem can be considered typical of the eastern Pacific Ocean boundary layer just outside of the equator (i.e., the equatorial undercurrent is not included). Because the integration is relatively short (1 day), the inclusion of rotation at low latitudes would not have much effect on the results. Although not encompassing a wide range of oceanic conditions, the test problem does cover the growth and decay of convective turbulence and shear-driven turbulence, which are the main ingredients of diurnal cycling oceanic boundary layers at many parts of the world oceans. Domain size and horizontal and vertical resolution all vary by an order of magnitude. This study is a first step toward systematically assessing the robustness of ocean large-eddy simulations. It also serves as a reference for future convergence studies.

This paper is organized as follows. The LES model and numerical experiments are described in section 2. The diurnal cycling boundary layer and TKE budget are described in section 3. Sensitivity to domain size, horizontal resolution, and vertical resolution are discussed in section 4. Some concluding remarks are made in section 5. To provide readers with a perspective on the relative sensitivity of the LES model to resolution and to SGS parameterization, we describe the sensitivity of the LES model to the particular SGS model used in Appendix A.

2. LES Model and Numerical Experiments

The LES model used in this study was developed by *Moeng* [1984]. The governing equations of the LES model are

$$\mathbf{u}_t + \mathbf{u}\cdot\nabla\mathbf{u} = -\nabla p - \alpha\mathbf{g}T + \nabla\cdot\boldsymbol{\tau}, \tag{1}$$

$$\nabla\cdot\mathbf{u} = 0, \tag{2}$$

$$T_t + \mathbf{u}\cdot\nabla T = \nabla\cdot\mathbf{q} + \frac{1}{C_p}\partial_z I(t,z), \tag{3}$$

$$e_t + \mathbf{u}\cdot\nabla e = \boldsymbol{\tau}:\nabla\mathbf{u} - \alpha g q_3 - \epsilon + \nabla\cdot(2\kappa_m\nabla e), \tag{4}$$

$$\boldsymbol{\tau} = \kappa_m\left(\nabla\mathbf{u} + (\nabla\mathbf{u})^T\right),\ \mathbf{q} = \kappa_h\nabla T,\ \epsilon = c_\epsilon\frac{e^{3/2}}{l_\epsilon}, \tag{5}$$

where $C_p = 4.1\times10^6$ J m^{-3}K^{-1} is the specific heat of sea water per unit volume and $\alpha = 0.00028K^{-1}$ is the thermal expansion coefficient. The eddy viscosity and diffusivity coefficients are defined by

$$\kappa_m = c_k l\sqrt{e},\quad \kappa_h = c_h l\sqrt{e}. \tag{6}$$

The numerical constants in (5) and (6) are

$$c_k = \left(\frac{2}{3K_O}\right)^{3/2}\frac{1}{\pi} = 0.0856,$$

$$c_h = \left(\frac{2}{3K_O}\right)^{1/2}\frac{4}{3\gamma}\frac{1}{\pi} = 0.204,$$

$$c_\epsilon = \left(\frac{2}{3K_O}\right)^{3/2}\pi = 0.845,$$

where $K_O = 1.6$ and $\gamma = 1.34$ are Kolmogorov and Batchelor constants, respectively, for isotropic homogeneous turbulence [see *Schumann*, 1991]. Note that Kolmogorov and Batchelor constants are theoretically derived and are consistent with estimates from laboratory measurements. The only tunable variables of the SGS model are the subgrid lengthscales l_ϵ and l, defined as

$$l_\epsilon = \Delta, \tag{7}$$

$$l = \Delta\left[1 + c_l\frac{\overline{N^2}\Delta^2}{e}\mathrm{H}(\overline{N^2})\right]^{-1},\quad \text{for}\quad z < z_o, \tag{8}$$

$$l = \Delta\left[1 + 0.016\frac{(\overline{u_z}^2 + \overline{v_z}^2)\Delta^2}{e}\mathrm{H}(\overline{N^2})\right]^{-3/2},\quad \text{for}\quad 0 > z \geq z_o, \tag{9}$$

where $\Delta = (\Delta x\Delta y\Delta z)^{1/3}$ and $\overline{N^2} = \alpha g\overline{T}_z$. Overbars represent horizontal averages, H is the Heaviside step function, $c_l = 1.2$, and $z_o = -3$ m.

Absorption of solar radiation $I(t,z)$ is defined for moderately clear type IB water [*Jerlov*, 1968; *Paulson and Simpson*, 1977]:

$$I(t,z) = I_0\sin(\frac{2\pi}{P}t + \psi)\,\mathrm{H}\left[\sin(\frac{2\pi}{P}t + \psi)\right]\cdot[0.6\exp(z/\lambda_1) + 0.4\exp(z/\lambda_2)], \tag{10}$$

where I_0 is the local noon solar irradiance, $P = 1$ day is the diurnal period, $\lambda_1 = 1$ m, and $\lambda_2 = 17$ m. The constant ψ is the initial phase of integration. For example, if the integration starts at sunset, $\psi = -pi$.

The LES model is forced with a constant wind stress $\tau_x = -0.02$ Nm^{-2} (easterly) and diurnal cooling and heating, represented by a constant cooling rate of $Q = -200$ Wm^{-2} and a sinusoidal daytime heating with a noon irradiance of $I_0 = 300\pi$ Wm^{-2}. The daily averaged equivalent surface heat flux is 100 Wm^{-2}. The initial stratification is typical of the eastern equatorial Pacific near 140°W, with an initial mixed layer depth of 17.5 m, defined as the depth at which density differs from that of the surface by 0.01 kgm^{-3}. Buoyancy frequency varies from zero in the top 8 m to 0.011 s^{-1} at the bottom of the model domain. The initial conditions consist of a horizontally uniform temperature

Table 1. Numerical Experiments[a]

Number	Name	Grid Geometry	Resolution, m	Domain Size, m	Times Step, s	Cost, %
1	Control	192 × 192 × 140	$\Delta x = \Delta y = 0.5$, $\Delta z = 0.50$	$L_x = L_y = 96$	0.5	100.00
2	DS1	16 × 16 × 70	$\Delta x = \Delta y = 1.0$, $\Delta z = 1.00$	$L_x = L_y = 16$	1.0	0.17
3	DS2	32 × 32 × 70	$\Delta x = \Delta y = 1.0$, $\Delta z = 1.00$	$L_x = L_y = 32$	1.0	0.69
4	DS3	64 × 64 × 70	$\Delta x = \Delta y = 1.0$, $\Delta z = 1.00$	$L_x = L_y = 64$	1.0	2.78
5	DS4	128 × 128 × 70	$\Delta x = \Delta y = 1.0$, $\Delta z = 1.00$	$L_x = L_y = 128$	1.0	11.11
6	HR1	16 × 16 × 70	$\Delta x = \Delta y = 6.0$, $\Delta z = 1.00$	$L_x = L_y = 96$	6.0	0.03
7	HR2	32 × 32 × 70	$\Delta x = \Delta y = 3.0$, $\Delta z = 1.00$	$L_x = L_y = 96$	3.0	0.23
8	HR3	64 × 64 × 70	$\Delta x = \Delta y = 1.5$, $\Delta z = 1.00$	$L_x = L_y = 96$	1.5	1.85
9	HR4	96 × 96 × 70	$\Delta x = \Delta y = 1.0$, $\Delta z = 1.00$	$L_x = L_y = 96$	1.0	6.25
10	VR1	64 × 64 × 35	$\Delta x = \Delta y = 1.0$, $\Delta z = 2.00$	$L_x = L_y = 64$	1.0	1.39
11	VR2	64 × 64 × 70	$\Delta x = \Delta y = 1.0$, $\Delta z = 1.00$	$L_x = L_y = 64$	1.0	2.78
12	VR3	64 × 64 × 280	$\Delta x = \Delta y = 1.0$, $\Delta z = 0.25$	$L_x = L_y = 64$	1.0	11.11

[a]The domain size in the vertical is $L_z = 70$ m for all experiments. The acronyms DS, HR, and VR stand for horizontal domain size, horizontal resolution, and vertical resolution, respectively. Note that experiments DS3 and VR2 are the same experiment, listed twice here for ease of discussion on the sensitivity to vertical resolution. Computational cost is the CPU usage relative to the control run.

profile and a random horizontal velocity field of small amplitude at the top six levels. Below these levels, the initial velocity field is zero. The integration starts at sunset (or 6 pm). We arbitrarily denote time $=-6$ hours for the beginning of integration.

The numerical experiments are listed in Table 1. Experiment 1, which we shall call the control experiment, has the finest overall resolution of 0.5 m on a 96 m × 96 m × 70 m domain. In this study, domain size always means the horizontal domain size because the vertical extent of the domain is $L_z = 70$ m for all experiments. Although the control experiment might not be the highest resolution ocean LES experiment in terms of the number of grid points used, the computational cost is enormous because of the small time step (0.5 s, dictated by the small grid size) and the length of integration (about 1 day). It represents the state of the art of ocean LES today. In this study the solution of the control experiment serves as the "truth" by which all other experiments with either smaller domains or coarser resolutions are judged. Of course, the truth is relative because the real true solution might have to come from a direct numerical simulation or a laboratory experiment. The purpose of this study is to shed some light on how economical ocean LES should be conducted such that the solutions are reasonably convergent.

Experiments DS1-DS4 (i.e., experiments 2-5, Table 1) are designed to investigate the sensitivity of LES solutions to model domain size. These experiments have the same isotropic resolution of 1 m but have different domain sizes. Intuitively, the length in each direction of the model domain should be comparable to or larger than the mixed layer depth to resolve the largest eddies, which should have scales comparable to the mixed layer depth. To verify this assumption, we employ a smaller domain size in DS1, with $L_x = L_y = 16$ m, which are smaller than the maximum mixed layer depth at night (about 30 m). Compared to case DS1, the domain size for cases DS2, DS3, and DS4 increased by factors of 4, 16, and 64, respectively. Note that the domain size for experiment DS5 is 77% larger than that of the control case. Ideally, an experiment using this domain size and a 0.5 m resolution should be done and used as the reference or the truth. Because of the enormous computational cost, we did not conduct this experiment. This deficiency, however, does not change the conclusions we shall draw from this study.

Experiments HR1-HR4 (i.e., experiments 6-9, Table 1) are designed to investigate the sensitivity of LES solutions to horizontal resolution. The domain size for these four experiments is the same as that of the control experiment, i.e., 96 m × 96 m. The vertical resolution is $\Delta z = 1$ m for all four experiments. The horizontal resolutions are 6, 3, 1.5, and 1 m for HR1, HR2, HR3, and HR4, respectively. Note the horizontal resolution of the control experiment is one-twelfth that of HR1, or 0.5 m. Except in HR4 and the control experiment, the resolutions of HR1-HR3 are anisotropic. Namely, the horizontal grid sizes are larger than the vertical grid sizes, with aspect ratios of 6, 3, and 1.5, respectively. These experiments will shed some light on whether anisotropic resolutions can be used to obtain reasonable solutions.

Experiments VR1, VR2, and VR3 (i.e., experiments 10-12, Table 1) are designed to investigate the sensitivity to vertical resolution. All three experiments have the same horizontal resolution of 1 m. The vertical resolutions are 2.0, 1.0, and 0.25 m for VR1, VR2, and VR3, respectively. The vertical resolution varies by a factor of 8, or about an order of magnitude. Note that experiment VR2 is actually the same experiment as DS3 (experiment 4). It is listed twice in Table 1 to facilitate the discussion on sensitivity to vertical resolution and to avoid confusion (citing them as VR1, VR2, and VR3, instead of VR1, DS3, and VR3).

The computational costs of all experiments relative

to the control experiment are listed in the last column of Table 1. For a specific application (integration length in real time) and a given amount of computer time a coarser resolution has to be used if a larger domain size is employed. Conversely, when a smaller domain is used, the resolution can be increased, but the time step of integration has to be reduced accordingly because of the explicit time difference scheme used in the LES model. So, one needs to bear in mind the computational efficiency when discussing the qualities of simulations with fine resolutions on small domains versus simulations with coarser resolutions on large domains. If designed poorly, one might only obtain a small gain in accuracy at the expense of a huge increase in computational cost.

3. Solution of the Control Experiment

We briefly describe the control solution before moving on to the discussion of sensitivity issues because the solution itself might be of some value for future reference and for the validation of simple 1-D mixed layer models.

Plate 1 shows the evolution of (top) horizontally averaged temperature and (bottom) zonal velocity. The mixed layer depth, which is defined as the depth at which potential density differs from that of the surface by 0.01 kgm^{-3}, is also shown (white lines). During the night the mixed layer (white line) deepens gradually from a depth of 17.5 m at sunset to a depth of 31 m at 0700 LT with a deepening rate of roughly 1 mh^{-1}. The vertical profile of temperature at night can be divided into two parts on the basis of the sign of temperature gradient: (1) a super adiabatic layer (in the depth range 0-10 m) and (2) a stratified layer (below about 10 m). On the basis of the magnitude of the temperature gradient, it can be divided into three parts: (1) a cool surface layer with a strong negative temperature gradient, (2) a well-mixed layer, and (3) a stably stratified layer below. In the real ocean, there is another layer, the so-called cool skin layer, which is only a few millimeters thick near the surface. The model grid size (0.5 m) is not fine enough to resolve this cool skin layer. After sunrise (time > 6 hours) the mixed layer shallows from a depth of 31 m to a depth of 3 m in just 1 hour. Note, however, that the temperature is still relatively well mixed below the mixed layer a few hours after the sunrise. Restratification is fully established only in the late afternoon hours. The evolution of mixed layer depth, of course, depends on how the mixed layer is defined. If a different criterion is used, the rate of deepening and shallowing might be somewhat different. Note also that during the day, temperature gradient near the surface is still negative, but the super adiabatic layer is much thinner than at night. Zonal velocity shows similar characteristics as temperature. During convection the velocity profile can also be divided into three parts: (1) a surface shear layer, (2) a well-mixed layer, and (3) a sheared layer near the bottom of the mixed layer. After sunrise a strong surface current (diurnal jet) is developed, with maximum velocity occurring at about 1500 LT. Note that there is considerable shear inside the daytime mixed layer as well as below the daytime mixed layer. The implication for bulk mixed layer models is that the assumption of a uniform horizontal velocity inside the mixed layer is an oversimplification and might not be justified during strong solar heating.

We now turn to the turbulent kinetic energy (TKE) budget. The governing equation of TKE is

$$\frac{dTKE}{dt} = S + B + D + T + P, \tag{11}$$

where

$$S = - < u'w' > \frac{\partial U}{\partial z},$$

$$B = \alpha g < w'T' >,$$

$$D = -\epsilon,$$

$$T = -\frac{\partial}{\partial z} < (u'u' + v'v' + w'w')w' >,$$

$$P = -\frac{\partial < pw >}{\partial z}$$

are shear production, buoyancy production (or buoyancy destruction, when it is negative), dissipation, turbulent transport, and pressure transport of the TKE, respectively. Here triangle brackets stand for horizontal average, U is the horizontally averaged zonal velocity, and (u', v', w') are velocity fluctuations, or deviations from the horizontal mean.

Figure 1 shows the TKE budget. During the night (Figure 1a), buoyancy production (B, thin solid line) is the major source of turbulence above 15 m, as a result of the surface cooling. It is a sink term below about 20 m. Shear production (S, thick solid line) is much stronger than buoyancy production near the surface and is significant near the bottom of the boundary layer (near 30 m) compared to buoyancy production but is insignificant for the rest of the boundary layer. Turbulent transport (T, dotted line) is a sink of turbulence near the surface and is the dominant source of turbulence below 15 m, except near the bottom of the boundary layer, where it is comparable to shear production. Pressure transport (dot-dashed line) is a source of turbulence near the surface and near the bottom of the boundary layer but is a sink in between. Note that turbulent transport and pressure transport tend to cancel each other. Overall, TKE balance at night is basically that of convection except near the surface and at the bottom of boundary layer, where shear production is important.

During the day, TKE balance is basically that of shear-driven turbulence in the top 8 m (Figure 1b), where shear production is the dominant source of turbulence. Buoyancy production is an insignificant source of turbulence near the surface and is a sink in the depth range 1-7.5 m. Again, turbulent transport and pres-

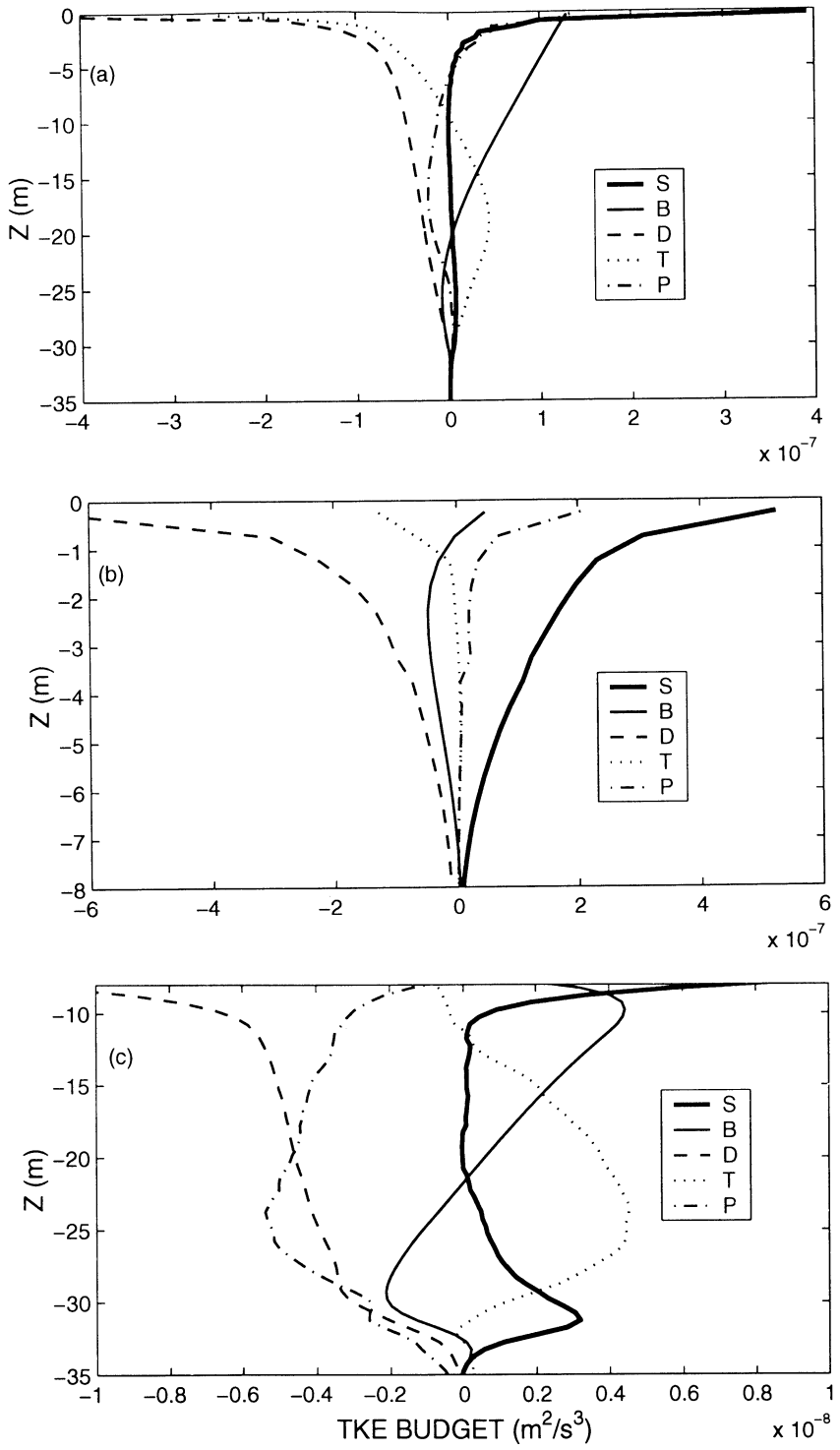

Figure 1. TKE budget (a) averaged at night, (b) averaged during the day for the depth range 0-10 m, and (c) averaged during the day for the depth range 10-35 m. S, B, D, T, P stand for shear production, buoyancy production, dissipation, turbulent transport, and pressure transport, respectively. The time rate of change is very small relative to other terms and is not shown. See text for details.

sure transport tend to cancel each other, similar to the nighttime balance. Crudely, the TKE balance can be approximated by a balance between shear production, buoyancy production, and dissipation during the day above 8 m. During the day below 8 m (Figure 1c), the TKE balance is that of a decaying convective turbulence with a contribution of shear production near the bottom of the boundary layer. Note that the range of abscissa in Figure 1c is much smaller than that of Figure 1b. The source terms are shear production, buoyancy production (for the depth range 8-22 m), and turbulent transport. The sink terms are buoyancy destruction (below

22 m), pressure transport, and dissipation. The complicated transition from shear-driven turbulence near the surface to decaying turbulence well below the mixed layer poses a challenge for simple 1-D mixed layer models.

In the discussion of sensitivity issues we shall not compare the TKE balances of the other experiments with that of the control experiment because of the large number of experiments involved. Instead, we only focus on a few turbulent statistics such as TKE, dissipation, heat flux, and momentum fluxes. Since we found that mean fields such as shear and stratification are relatively insensitive to domain size and resolution, the differences in the turbulent statistics we shall show reflect the differences in TKE balances.

4. Sensitivity to Domain Size and Resolution

The choice of domain size and resolution of an LES experiment depends on several factors. First, the domain size should be large enough that the largest eddies in the boundary layer are resolved and that further increase in domain size does not result in very different solutions (here we mean statistics of mean fields and second moments). Second, the resolution should be fine enough that further increase of resolution does not change the turbulent statistics significantly. Third, when computational cost comes into play, one has to balance the above two factors. Is it better to sacrifice resolution so a larger domain size can be used or is it better to sacrifice domain size so a finer resolution can be used for a given amount of computer time? The answer, of course, depends on how sensitive LES solutions are to domain size and resolution.

4.1. Sensitivity to Domain Size

Experiments DS1-DS4 (Table 1) have the same resolution but have different horizontal domain sizes, varying from 16 m × 16 m in DS1 to 128 m × 128 m in DS4, or a factor of 64. Figure 2 shows vertical profiles of TKE, dissipation, heat flux, and momentum flux averaged for the night. The control solution is also shown for comparison (thick solid lines). For domain size DS1, TKE is significantly smaller than those of the experiments with larger domains (Figure 2a, thin solid line). Turbulent dissipation also significantly differs from the rest of the experiments (Figure 2b). Entrainment heat flux (negative extremum near 25 m in Figure 2c, thin solid line) is also significantly less than those of other domain size experiments. The same is true for momentum flux (Figure 2d, thin solid line). For domain size DS2, TKE is significantly smaller than those of DS3 and DS4 above 10 m (Figure 2a, dashed line). However, dissipation, heat flux, and momentum flux are not very different (Figure 2b-2d). It is apparent that domain size DS1 is too small and DS2 is marginally acceptable. Experiments DS3 and DS4 show very small differences above 30 m; namely, convergence is more or less achieved at domain size DS3. For nighttime convection we conclude that each dimension of the horizontal domain size should be at least twice that of the boundary layer depth, although domain size comparable to the mixed layer depth is still useful if computer resources are severely limited. Note that below the boundary layer (below 30 m), there is a tendency of increasing momentum flux (more negative) as the domain size increases (Figure 2d, below 30 m). For example, the downward momentum flux of DS2 is 3 times that of DS1 (compare dashed line and thin solid line, Figure 2d). The downward momentum fluxes of DS3 and DS4 (Figure 2d, dotted and dot-dashed lines) are 30% higher than that of DS2 (dashed line). Although DS2 is acceptable as far as heat flux and momentum flux are concerned inside the boundary layer, it might not be acceptable if fluxes into the deep ocean are concerned.

Figure 3 shows daytime averages of vertical profiles of TKE, dissipation, heat flux, and momentum flux. TKE tends to increase as the domain size is increased (Figure 3a). For example, TKE of DS4 is significantly larger than those of DS1 through DS3. The largest differences among domain size cases, in terms of percentage, occur below 15 m. TKE of DS2 and DS3 is about twice that of DS1, and the TKE of DS4 is about 30% larger than those of DS2 and DS3. Obviously, the solution is more sensitive to domain size during the day than during the night. Unlike the nighttime average, the TKE of DS1-DS4 is very different from that of the control solution above 15 m. Most notably, the local extrema at 5 m seen in DS1-DS3 are absent in the control solution. This is due to the fact that the control experiment has a finer resolution.

Differences in turbulent dissipation among different cases are not as striking as in TKE (Figure 3b), but larger differences are seen below 30 m. The smallest domain size case DS1 has the smallest dissipation rate. Note that turbulence dissipation of experiments DS1-DS4 differs from that of the control experiment significantly in the depth range 8-15 m. Again, this is due to the fact that the control experiment has a finer resolution. Heat fluxes of different cases do not show much difference above 10 m (Figure 3c). The same is true for momentum flux (Figure 3d). Below 10 m both heat flux and momentum flux show large differences in percentage terms. In absolute terms however, the differences are rather small.

From the results discussed above it is apparent that TKE is more sensitive to domain size than are heat flux and momentum flux. There are two reasons for this. First, heat flux and momentum flux at the surface are prescribed. Namely, at the surface the resolved fluxes are zero (because $w = 0$) and the SGS fluxes are the total fluxes. Right below the surface, fluctuations of vertical velocity w are small because of the constraint of the bounding surface. This results in smaller fluxes due to resolved motions. In other words, SGS fluxes contribute significantly to the total fluxes near the surface.

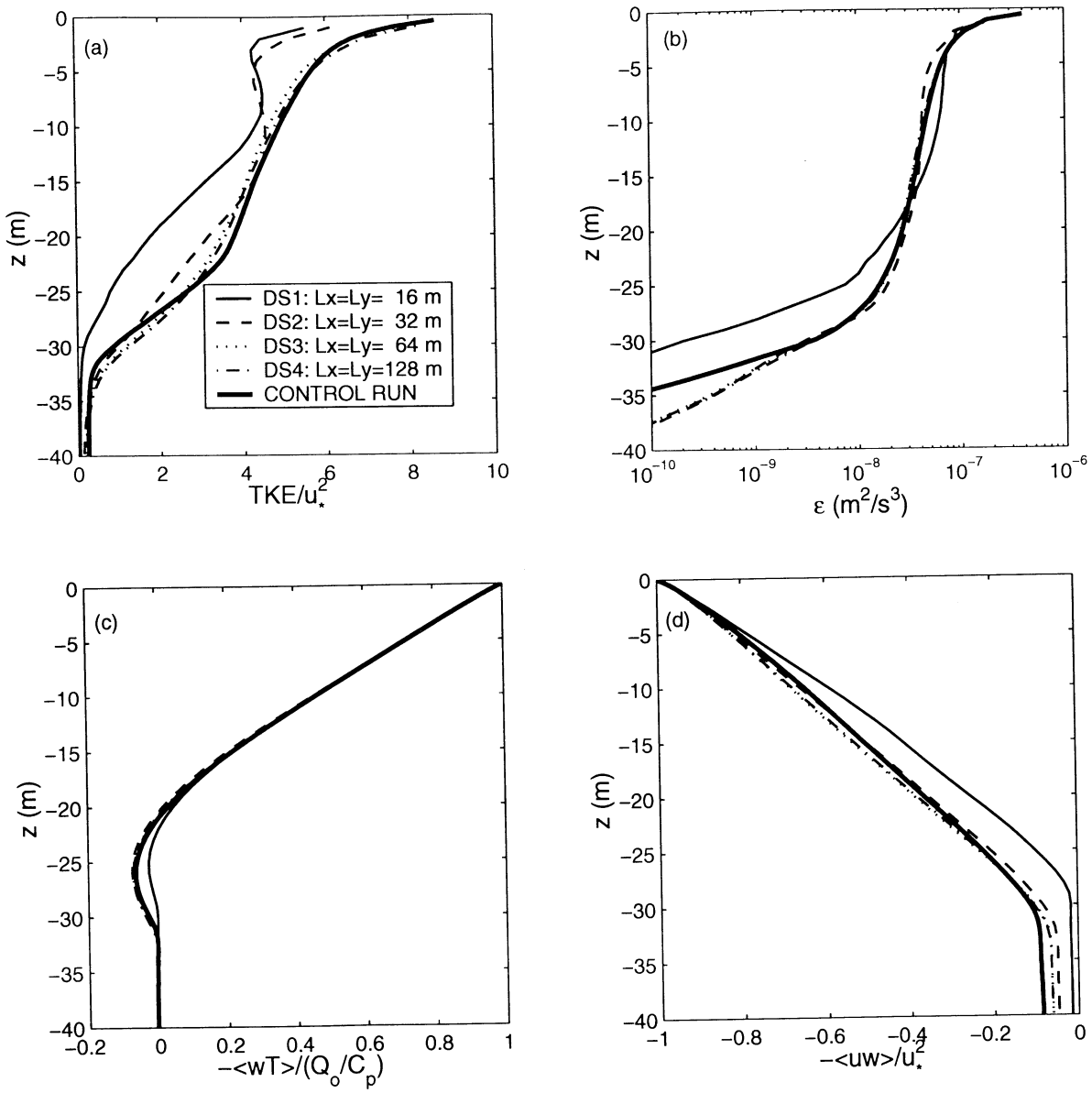

Figure 2. Nighttime average of (a) TKE, (b) dissipation, (c) heat flux, and (d) momentum flux for the domain size experiments (thin lines) and the control run (thick solid lines). TKE and momentum flux are normalized by u_*^2, where $u_* = 0.0044$ ms^{-1}. The heat flux is normalized by the surface cooling rate $Q_0 = -200$ Wm^{-2}.

The same is true for SGS TKE. Furthermore, there is no constraint on the value of the SGS TKE itself because of the zero-gradient boundary condition used. (In future studies the validity of this zero-gradient boundary condition for SGS TKE should be reexamined. Perhaps, a formulation relating the surface value of SGS TKE to resolution and surface forcing is needed.) Second, the autocorrelation of a variable is, in general, larger than the cross correlation with a different variable. An example is that internal waves carry momentum fluxes but no heat fluxes. In the entrainment layer (the region below the mixed layer but above the depth at which turbulent heat flux is practically zero), turbulence is intermittent, and what we call TKE here actually contains internal wave energy. Below the boundary layer, the variable TKE is entirely that of kinetic energy of internal waves, which tend to have much larger scales than turbulence. This is the reason that below the boundary layer, momentum flux is more sensitive to domain size than is heat flux (compare Figure 2c and Figure 2d).

4.2. Sensitivity to Horizontal Resolution

Experiments HR1-HR4 (Table 1) and the control experiment have the same domain size of 96 m × 96 m, but have different resolutions. The horizontal resolution varies from 6 m in DS1 to 0.5 m in the control case, or a factor of 12. The vertical resolution is 1 m for experiments HR1-HR4 and 0.5 m for the control ex-

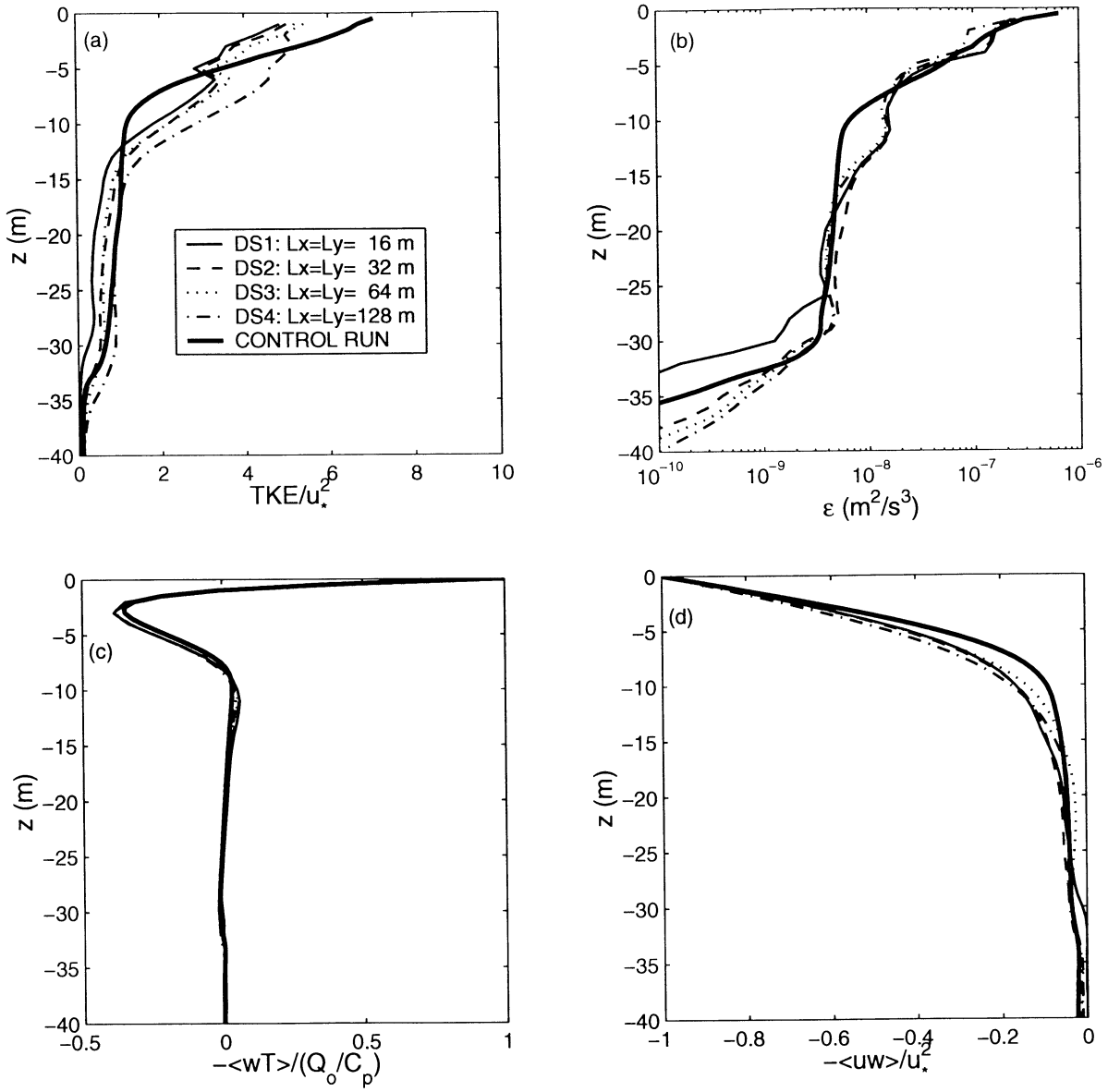

Figure 3. Same as Figure 2 except for daytime average.

periment. Figure 4 shows vertical profiles of nighttime and daytime averages of TKE and heat flux. During the night, there is a tendency of decreasing TKE when horizontal resolution is increased (Figure 4a). Convergence is essentially achieved at the horizontal resolution of 1.5 m (HR4). During the day (Figure 4b), there are significant differences between experiments HR1-HR4 and the control experiment. Note, for example, that the control solution does not exhibit the local extrema seen in experiments HR1-HR4. As found earlier from domain size experiments, heat fluxes during the night (Figure 4c) and during the day (Figure 4d) only show small differences among different experiments. For example, the entrainment heat fluxes (negative extrema at 25 m in Figure 4c and at 3 m in Figure 4d) of HR1-HR4 and of the control experiment do not differ from each other by more than 10%. Dissipation and momentum flux show similar differences in domain size cases (not shown). The conclusion is that TKE is more sensitive to horizontal resolution than are the turbulent fluxes. As far as TKE is concerned, convergence is not achieved at 1 m resolution for daytime shear-driven turbulence.

To examine further the sensitivity of LES solutions to horizontal resolution, we show in Figure 5 vertical profiles of resolved and SGS heat fluxes of HR1-HR4 and the control experiment averaged for the night. A few meters below the surface, resolved heat fluxes dominate the SGS fluxes (resolved fluxes are represented by thick lines and SGS fluxes are represented by thin lines). As the horizontal resolution increases, resolved heat flux increases modestly but SGS flux decreases dramatically, in terms of percentage changes. For example, at 5 m the resolved heat flux only decreased 10% from HR4 to HR1 (compare thick dot-dashed and dashed lines, Figure 5)

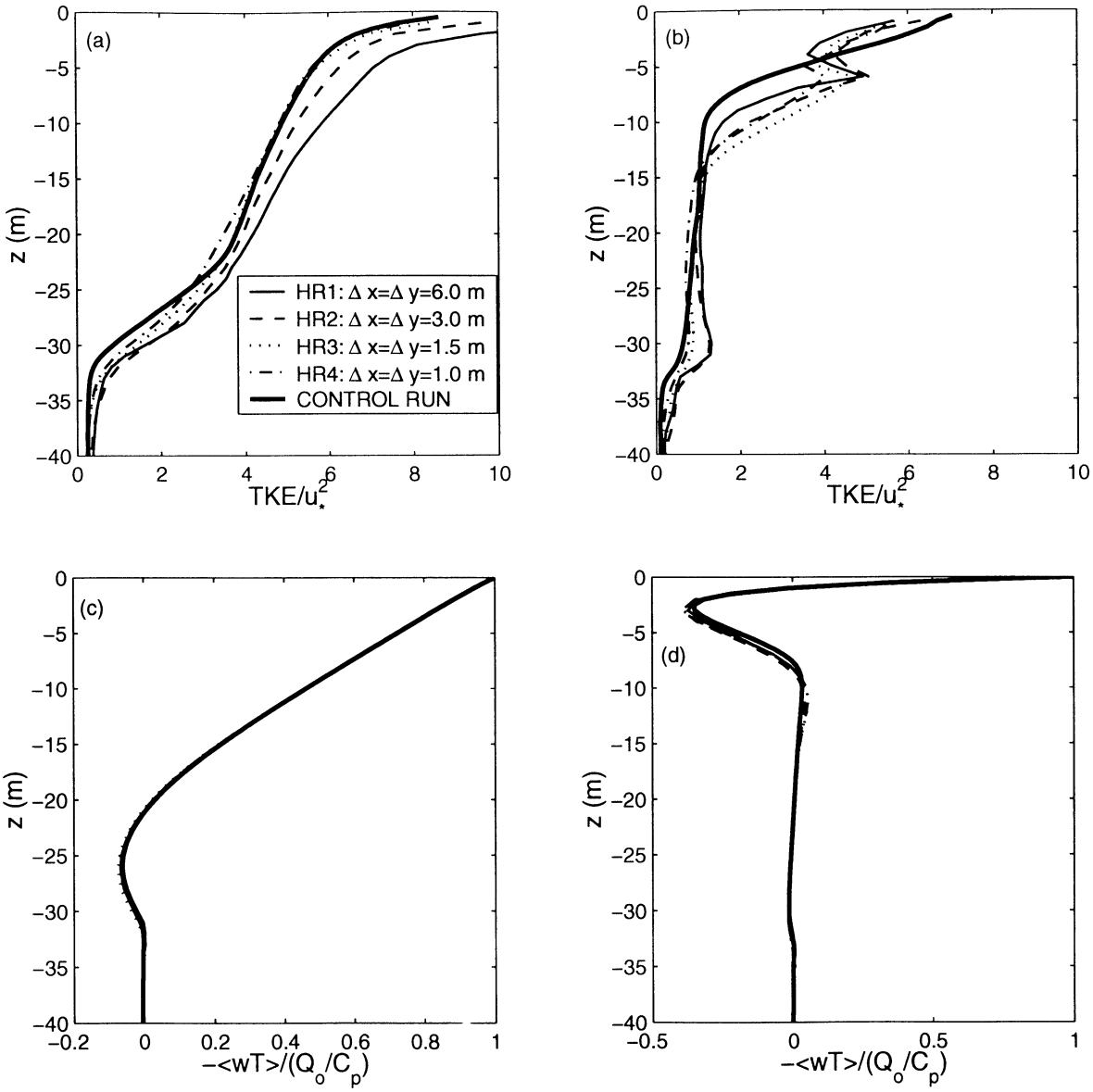

Figure 4. Nighttime average of (a) TKE and (b) heat flux and daytime average of (c) TKE and (d) heat flux for the horizontal resolution experiments (thin lines) and the control run (thick solid lines).

while the SGS flux increased by an order of magnitude (compare thin dot-dashed and dashed lines). Below 10 m, SGS fluxes are negligibly small for all experiments. As a result, total heat flux remains little changed for each experiment (see Figure 4c), that is, total heat flux is insensitive to horizontal resolution.

In the context of large-scale ocean circulation and climate research the major variables of interests in the oceanic boundary layer are surface velocity, temperature, and mixed layer depth. In Figure 6 we show the time series of surface temperature and mixed layer depth for the horizontal resolution experiments (surface velocity shows similar differences among different experiments, so it is not shown here). During the night (hours -6 to 6) and in the early hours after sunrise (hours 6-12), surface temperature (Figure 6a) and mixed layer depth (Figure 6b) of all experiments do not differ very much from each other. Larger differences are seen in the early afternoon hours. However, even these differences are small considering the diurnal ranges of surface temperature and mixed layer depth. Even the coarsest resolution case HR1 is acceptable, as far as surface temperature and mixed layer are concerned.

One of the premises of LES is that a significant portion of the inertial subrange (-5/3 law) of turbulence is resolved such that the parameterization of the SGS is only for the inertial subrange, which is more universal than the large eddies. To see how this assumption is met under different resolutions, we compare in Figure 7 nighttime power spectral densities (PSDs) of vertical velocity of the horizontal resolution experiments with that of the control experiment at 5, 10, 15, and 25 m. Sig-

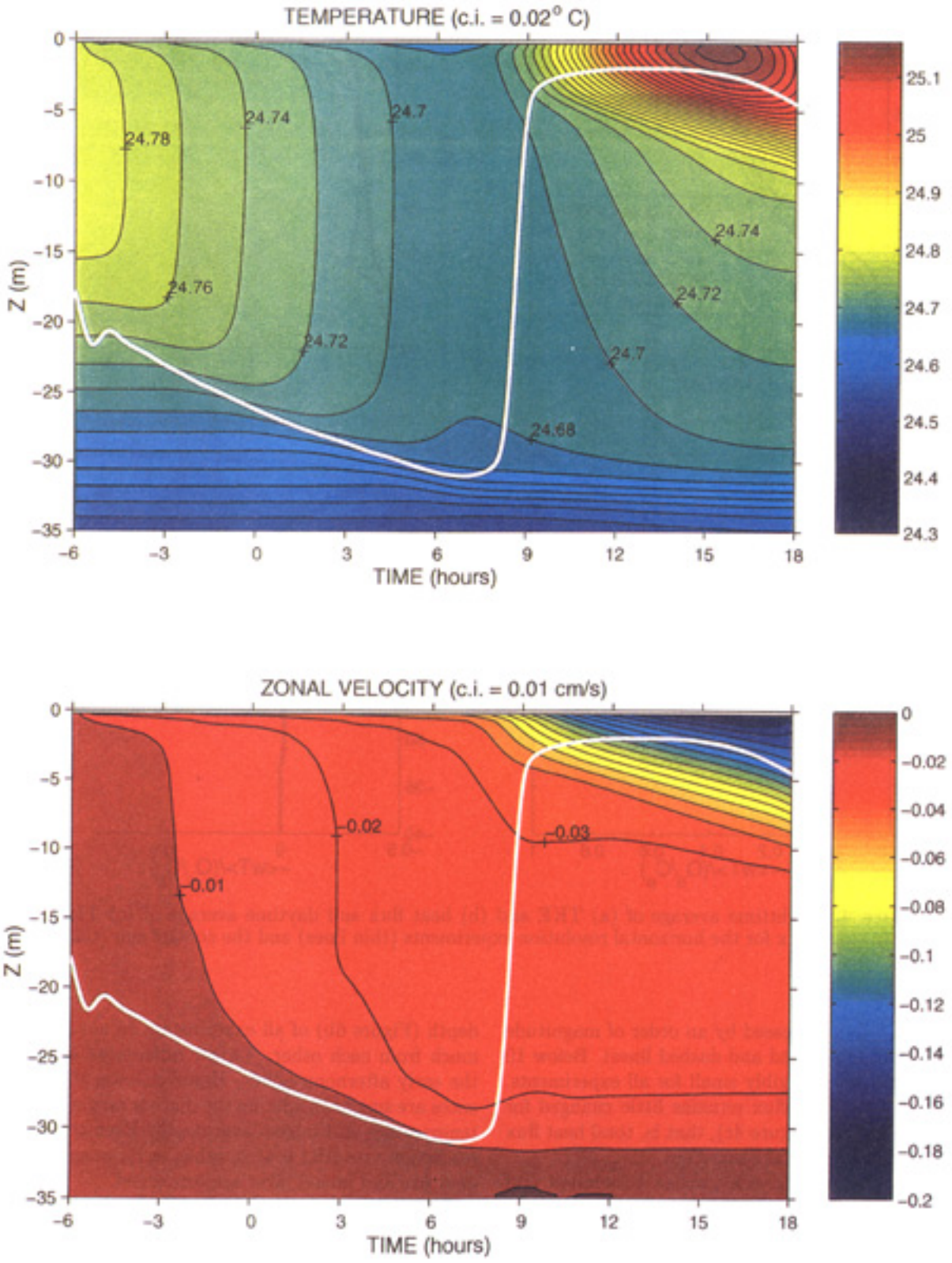

Plate 1. Time series of horizontally averaged (top) potential temperature (°C) and (bottom) zonal velocity (ms^{-1}) of the control experiment. The white lines represent the depth of the mixed layer depth, defined as the depth at which potential density differs from that of the surface by 0.01 kgm^{-3}. Time axis starts from 1800 LT, represented by -6.

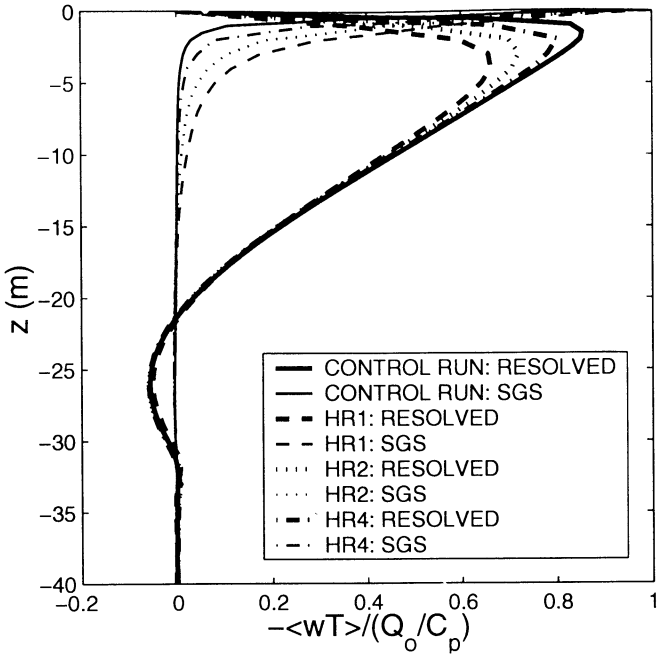

Figure 5. Resolved (thick lines) and SGS (thin lines) heat fluxes of control run, HR1, HR2, and HR4.

nificant portions of the PSDs of HR3 ($\Delta x = \Delta y = 1.5$ m, dotted lines), HR4 ($\Delta x = \Delta y = 1.0$ m, dot-dashed lines), and the control experiment at these depths are in the inertial subrange, as indicated by the -5/3 slope. For HR1 ($\Delta x = \Delta y = 6.0$ m, thin solid lines) the PSD does not contain an inertial subrange at these depths, except that one can probably argue that PSD at the highest wave number end catches a small portion of the inertial subrange at the depth of 25 m. For HR2 ($\Delta x = \Delta y = 3.0$ m, dashed lines), the PSD does not exhibit an inertial subrange at 5 and 10 m but does exhibit an inertial subrange at 15 m and 25 m. A few meters below 25 m, none of the HR experiments exhibit an inertial subrange; only the control case has an inertial subrange (not shown). Despite the fact that HR1 does not have a significant portion of the PSD in the inertial subrange, the turbulent fluxes are actually better than those of experiment DS1, which has a smaller domain but a much finer horizontal resolution of 1 m versus 6 m in HR1 (compare Figure 2c and Figure 4c). This underlines the importance of resolving the large eddies.

Most of the HR experiments (except HR1) also contain an inertial subrange during the early hours of decay and onset of nighttime convection. In the early afternoon hours however, none of the experiments, including the control experiment, contains an inertial subrange inside the shallow mixed layer, although resolved fluxes dominate SGS fluxes for the high-resolution experiments (HR3, HR4, and control). However, the total fluxes do not differ very much from those of the high-resolution experiments. If one insists that resolving a portion of the inertial subrange is essential at all times, the LES model has failed at the 0.5 m resolution. We would like to argue that this is not a big problem in practice. The overall diurnal cycle is still intact (Figure 6). With a much higher resolution such that the inertial subrange is resolved one might find that the maximum daytime surface temperature is different than those shown in Figure 6 in the early afternoon hours. At other times, however, it will closely follow the curves shown in Figure 6. We found that after sunset, the differences among different resolution cases diminished, suggesting further increase of resolution will not change the overall diurnal cycle very much. Nevertheless, we do not have confidence that the details of the 3-D struc-

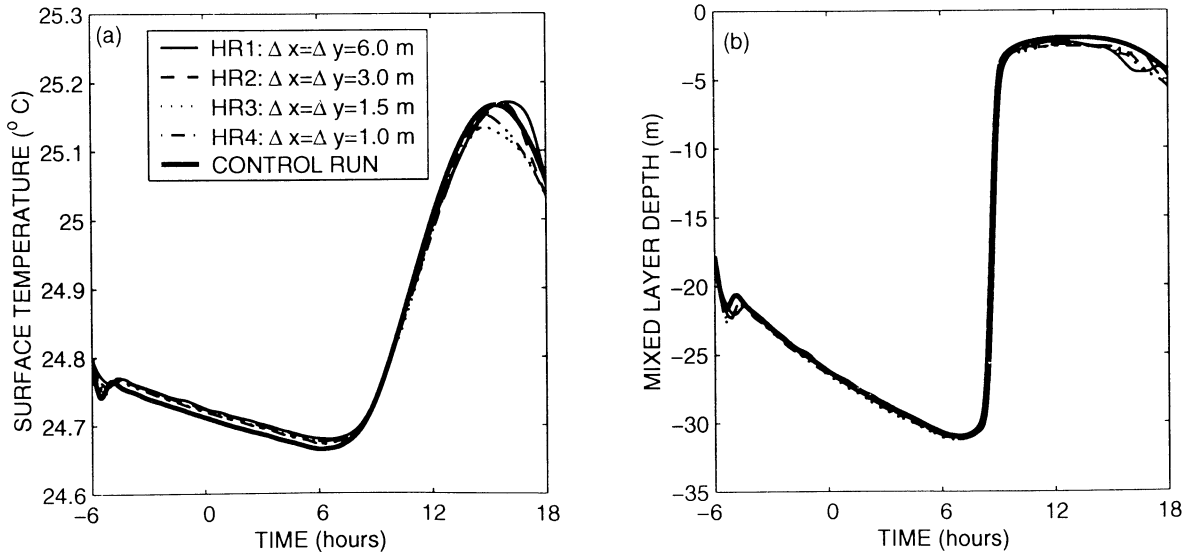

Figure 6. Time series of (a) surface temperature and (b) mixed layer depth for the horizontal resolution experiments (thin lines) and the control run (thick solid lines). The time axis starts from 1800 LT, represented by -6 hours.

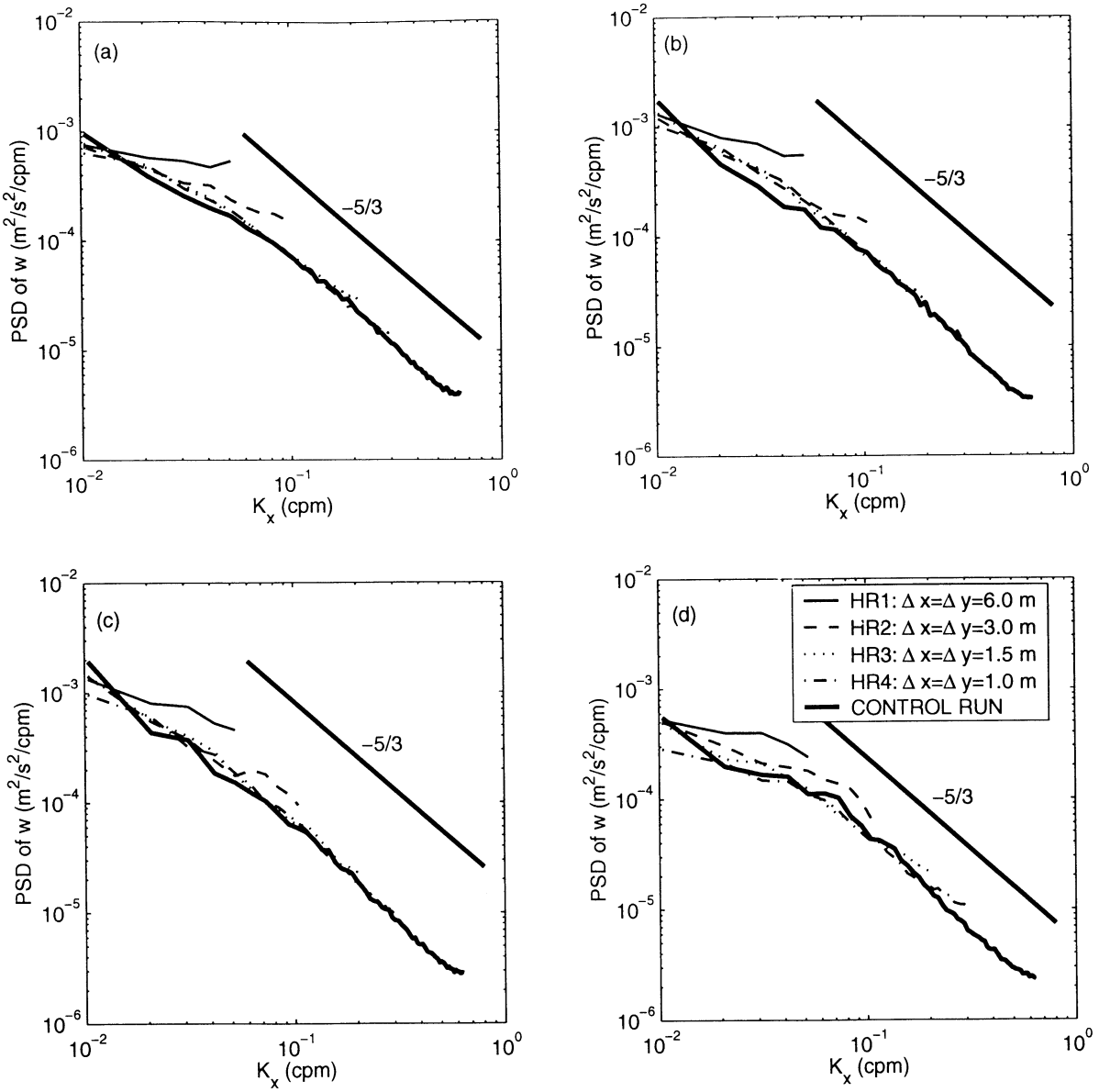

Figure 7. Power spectral densities of vertical velocity at (a) 5, (b) 10, (c) 15, and (d) 25 m for the horizontal resolution experiments HR1 (thin solid lines), HR2 (dashed lines), HR3 (dotted lines), HR4 (dash-dotted lines), and the control run (thick solid lines).

ture of turbulence in the early afternoon hours are well resolved for the control experiment because of the absence of an inertial subrange.

4.3. Sensitivity to Vertical Resolution

Experiments VR1, VR2, and VR3 (Table 1) have the same domain size of 64 m × 64 m and the same horizontal resolution of 1 m, but have different vertical resolutions of 2, 1, and 0.25 m, respectively. Figure 8 shows nighttime and daytime averages of the vertical profiles of TKE. At night, TKE is insensitive to vertical resolution; all cases are very close to the control solution (Figure 8a). During the day, however, TKE is sensitive to vertical resolution. Away from the surface, as the vertical resolution increases, TKE decreases. Near the surface this trend is not observed for VR3, which has the highest TKE. Convergence is obviously not achieved near the surface. Below about 3 m, VR3 and the control case are very close despite that fact that the horizontal resolution for VR3 is 1 m versus 0.5 m in for the control experiment, suggesting convergence at 0.5 m vertical resolution. This also suggests that the differences in TKE between the domain size experiments and the horizontal resolution experiments and the control solution seen in Figures 3a, 4a, and 8a are mainly due to the differences in vertical resolution. In other words, convergence is probably achieved at the control experiment resolution of 0.5 m, although we cannot verify this unless we conduct an even higher resolution experiment, which is beyond our capabilities at the present.

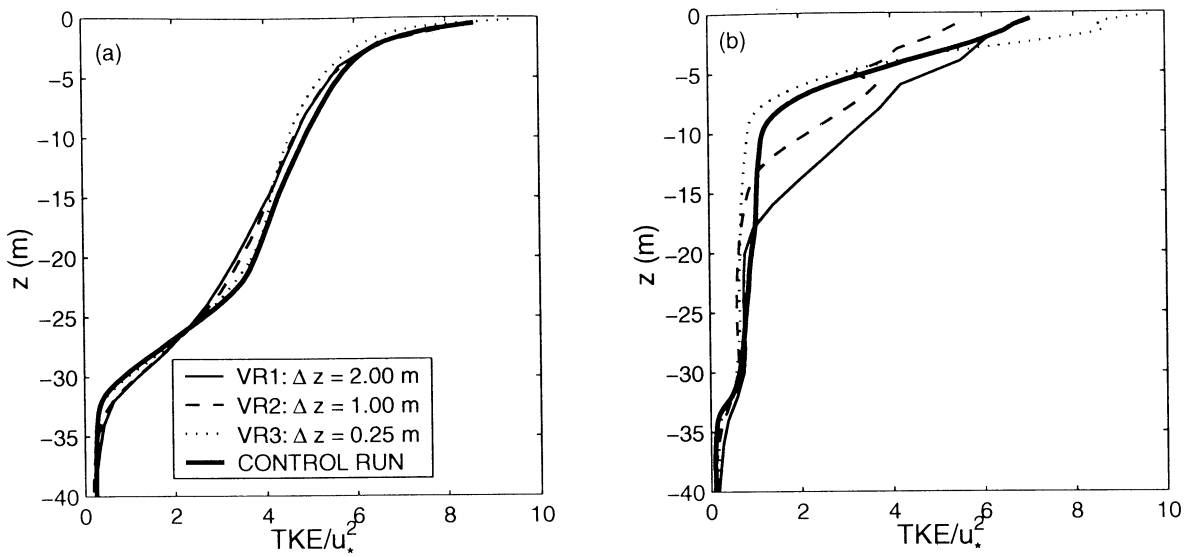

Figure 8. Vertical profiles of TKE at (a) nighttime and (b) daytime, for the vertical resolution experiments (thin lines) and the control run (thick solid lines).

Heat and momentum fluxes in general show smaller differences than does TKE and are comparable to those of domain size and horizontal resolution experiments (not shown).

For the problem considered here the timestep of integration is mainly determined by horizontal grid size and horizontal velocity. This is also true in the real ocean, where horizontal currents in the upper ocean are usually larger than the vertical currents. So, an increase in the horizontal resolution by a factor of 2 means an increase of computational cost by a factor of 8 (4 times more grid points with a timestep reduced by half). On the other hand, an increase in vertical resolution does not necessarily have to be accompanied a decrease in time step. Therefore the computational cost only increases linearly (until vertical resolution becomes the limiting factor of timestep). In other words, it is most economical to conduct LES experiments with a vertical resolution finer than the horizontal resolution. For example, the number of grid points for VR3 is 22% that of the control case, and the computational cost is only 11% that of the control case (Table 1) despite the fact that it has a finer vertical resolution. Furthermore, the solution is almost as good as the control solution, although the horizontal resolution is coarser (1 m in VR3 versus 0.5 m in the control experiment). Whenever computer resources are limited, one should emphasize adequate vertical resolution first before allocating the number grid points in the horizontal.

5. Discussion and Conclusion

A state-of-the-art oceanic large-eddy simulation experiment (high resolution and long integration) is conducted for a diurnal cycling oceanic boundary layer, forced by a constant wind stress and strong diurnal cooling and heating. During the night the solution is basically that of a convective boundary layer, although shear production is still the largest term in TKE budget near the surface. There is a super adiabatic layer with sharp gradients of temperature (negative) and velocity. Below this layer, there is a layer in which temperature and velocity are well mixed. The dominant terms in the TKE budget are buoyancy production, turbulent transport, pressure transport, and dissipation. Below this well-mixed layer, there is an entrainment layer in which turbulent transport and shear are the sources of turbulence. During the day the solution is basically that of a shear-driven stratified boundary layer, characterized by a TKE balance between shear production, buoyancy production/destruction, and dissipation.

It is impractical to conduct routinely long LES integrations with the same resolution of our control experiment to explore the dynamics of ocean mixed layers in different regimes. To address the questions whether small-domain or coarser-resolution LES experiments have any merits in the investigation of oceanic mixed layers and whether these experiments can be used to validate simple 1-D mixed layer models, we have conducted a series of experiments with various domain sizes and resolutions to investigate systematically the sensitivity of LES solutions to domain size and resolution, in the context of the diurnal cycling oceanic boundary layer of the control experiment. Domain size varied by a factor of 64, horizontal resolution varied by a factor 12, and vertical resolution varied by a factor of 8.

It is found that mean fields (temperature, mixed layer depth, and velocity) and turbulent fluxes are insensitive to domain size as long as the domain size is comparable to or greater than the mixed layer depth. However, each horizontal dimension of the domain size should be twice the mixed layer depth or larger to obtain robust

statistics of TKE, which tends to increase as domain size is increased.

Mean fields and turbulent fluxes are also insensitive to resolution, provided there are several vertical levels in the entrainment layer (e.g., $\Delta z = 1$ m for the depth range 25-30 m in Figure 2c). TKE however, shows varying degrees of sensitivity. Simulations with coarser resolutions tend to have larger values of TKE. Furthermore, TKE is more sensitive to domain size and resolution during the day (shear turbulence) than during the night (convection). For nighttime convection, convergence of TKE is essentially achieved at a horizontal resolution of 1.5 m. For daytime shear turbulence however, convergence of TKE is not achieved at a horizontal resolution 1 m (both horizontal and vertical). In conclusion, stably stratified shear turbulence demands much finer resolution than convective turbulence.

If computer resources are limited, a LES experiment with anisotropic resolution can be used, but the aspect ratio should not be ≥ 6 if vertical resolution only marginally resolves the entrainment layer. Preferably, the ratio is ≤ 3 (as in experiment HR2). With higher aspect ratios the inertial subrange can no longer be resolved. Of course, if the vertical resolution is very fine (as in experiment VR3), an aspect ratio of 6 or even larger might not be a problem.

An important finding of this study is that the resolution of large eddies is more important than the resolution of the inertial subrange of oceanic turbulence. With the same grid geometry of $32 \times 32 \times 70$ the solution of HR2 is better than that of DS1 (compare thin solid lines in Figure 2a and Figure 4a). The former has a larger domain size but has an anisotropic resolution with an aspect ratio of 3. The latter has a smaller domain but has an isotropic resolution (i.e., finer horizontal resolution), so the computational cost is 3 times that of the former. In other words, not only does HR2 provide a better solution, it is also cheaper to conduct. We should emphasize that only when computer resources are limited is anisotropic resolution with a larger domain preferred to isotropic resolution with a small domain. It is always better to have a large domain with an isotropic fine resolution such that a portion of the inertial subrange is resolved. It suffices to say that without the large eddies the LES model will fail, and without the inertial subrange, the LES model might or might not fail, for practical purposes.

On the basis of the above results we conclude that validations of simple 1-D mixed layer models using LES results with order $32 \times 32 \times 32$ resolutions are not without merit [e.g., Large and Gent, 1999] in the sense that mean fields and fluxes will not be much different if much higher resolutions are used. We should point out, however, that SGS fluxes contribute significantly to the total fluxes during the afternoon hours of daytime heating, for low-resolution experiments. The fact that the total fluxes turned out to be about right is an indication of the soundness of the SGS model. Of course, this can also be interpreted as a coincidence, from a conservative point of view. TKE from low-resolution experiments also shows large errors because it is more sensitive to resolution than are the fluxes. Therefore TKE from low-resolution experiments is not an appropriate variable to use for the validation of 1-D models. We should also point out that during intense solar heating the details of 3-D structure of turbulence are not resolved at coarse resolutions. Although the resolved fluxes dominate SGS fluxes for high-resolution experiments, the absence of an obvious inertial subrange in the early afternoon hours inside the mixed layer does not boost our confidence that the details of the 3-D structure of turbulence during these hours are correctly resolved. The mean fields and fluxes, however, will not be much different even if a much higher resolution is used. In other words, convergence does not necessarily mean the resolution of an inertial subrange.

Sensitivity to SGS parameterization is also an important issue in assessing the robustness of LES solutions. A systematic investigation of this sensitivity, however, is beyond the scope of the present study. To provide a perspective on how sensitive the LES model is to the SGS model relative to the sensitivity to resolution, we conducted several experiments to investigate whether the LES solutions are sensitive to the subgrid length scale of the SGS model. This length scale (equation (8)) is basically the only tunable variable of the SGS model. We found that the LES solution is less sensitive to the subgrid length scale than to the horizontal resolution. Furthermore, when resolution increases, the sensitivity decreases (see Appendix A for details). This is an attritute that any numerical model (LES models as well as ocean general circulation models) should posses. If not, the SGS model used is probably grossly incorrect.

The lack of surface wave processes is a drawback of this study. The real ocean surface is not a rigid lid. Langmuir circulation [*Langmuir*, 1938], caused by the interaction between surface gravity waves and wind driven currents, might be an important process contributing to the mixing of the upper ocean, although it is not the primary generation mechanism of oceanic mixed layers. We would expect that in the presence of Langmuir circulation, turbulence is enhanced near the surface. Therefore turbulence should be better resolved with a given resolution. In other words, the sensitivity to resolution should decrease in the presence of Langmuir circulation. On the other hand, if the horizontal scales of the Langmuir cells are large and the Langmuir cells contribute significantly to mixing, the LES solution might be more sensitive to domain size. These ideas need to be verified in the future.

Appendix A: Sensitivity to the Subgrid Lengthscale

The SGS model used in this study is a one-equation model for the evolution of the SGS TKE. The eddy diffusivity and viscosity coefficients are parameterized

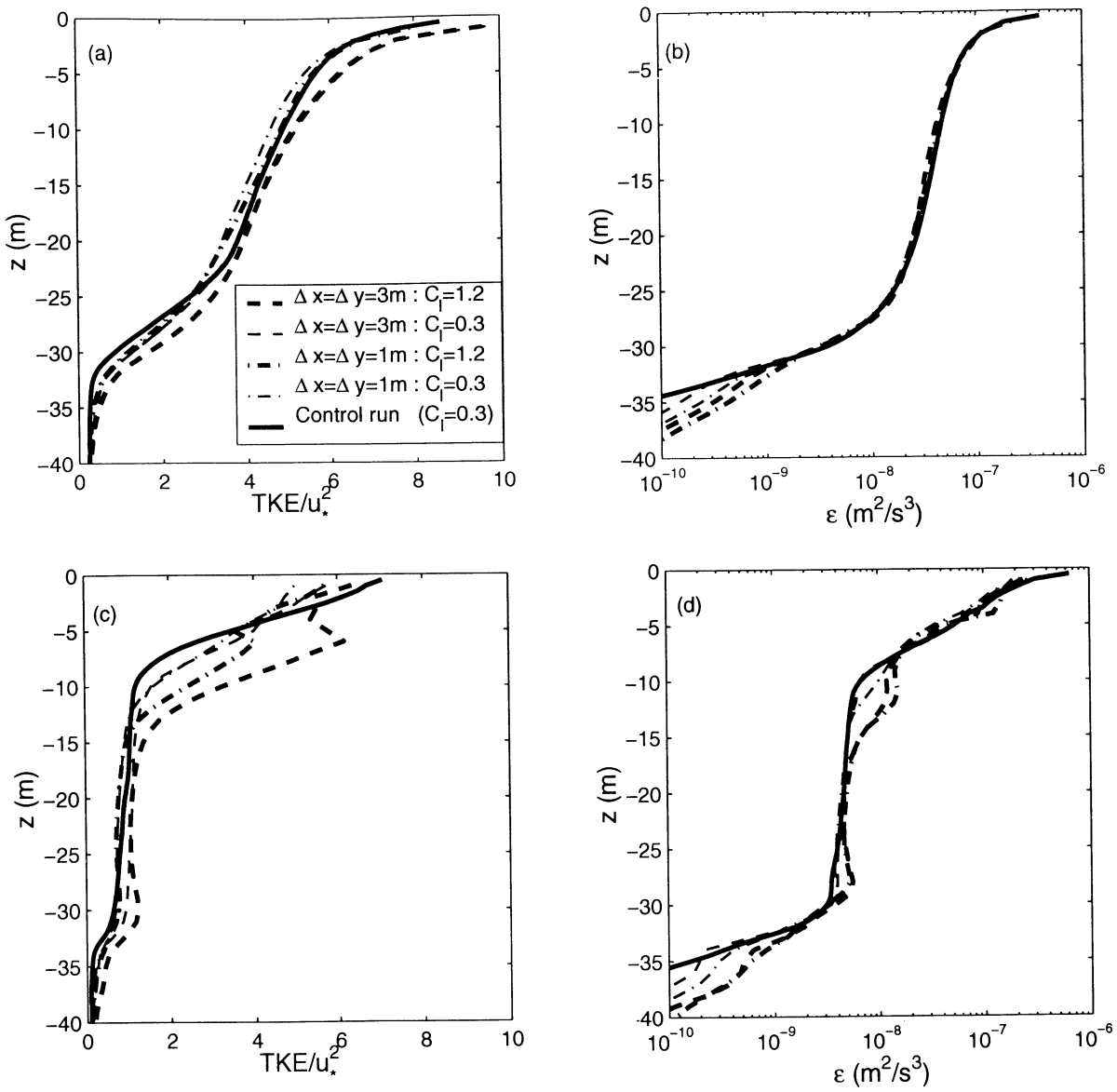

Figure 9. Night time average of (a) TKE and (b) dissipation and daytime average of (c) TKE, and (d) dissipation for the SGS experiments. Solution of the control experiment is also included for reference (thick solid lines).

through the introduction of a SGS lengthscale l, which is defined in (8)-(9). The lengthscale is a function of the SGS TKE, stratification, or shear. For convection (at night) it is only a function of the SGS TKE and stratification. For shear-driven turbulence, shear has an effect on the lengthscale near the surface. Our experience shows that (9) can be replaced by (8), provided some clipping of l is still applied near the surface (i.e., setting a minimum value of l to account for the so-called wall effect of shear turbulence see [*Wang et al.* 1996]. In essence, c_l in (8) is the only tunable parameter of the SGS formulation.

There are two limiting expressions for l. For neutral and unstable stratification the limit is $l = \Delta = (\Delta x \Delta y \Delta z)^{1/3}$, which is realized near the surface during nighttime convection. For strongly stably stratified fluid the limit is $l = e/(c_l N^2 \Delta^2)$, which can be realized below the mixed layer in the stratified region and near the surface during the day.

Schumann [1991] recommended $c_l = 0.3$ on the basis of *Weinstock* [1978]. On the basis of a recent work of *Weinstock* [1992], *Wang et al.* [1996] arrived at $c_l = 1.2$, which is the default value for the experiments in Table 1. In the strong stratification limit a change of $c_l = 1.2$ to $c_l = 0.3$ means an increase of the subgrid lengthscale l by a factor of 4. The sensitivity test of c_l consists of two pairs of experiments. In each pair, one experiment has $c_l = 1.2$, and the other has $c_l = 0.3$. The pairs differ in horizontal resolution and domain size. For the first pair the horizontal resolution is 3 m, with a grid geometry of 128 × 128 × 70. For the second pair, the horizontal resolution is 1 m, with a grid geometry of 96 × 96 × 70.

All experiments have the same vertical resolution of 1 m. The reason for using two horizontal resolutions is to test the hypothesis that as resolution increases, the sensitivity to SGS parameterization should decrease.

Figure 9 shows vertical profiles of TKE and dissipation averaged for the night and for the day, along with the control solution. At night, only slight differences in TKE are seen between cases of $c_l = 1.2$ and cases of $c_l = 0.3$ (compare thick and thin dashed lines at 3 m resolution; compare thick and thin dot-dashed lines at 1 m resolution). Obviously, the solutions are more sensitive to resolution than to c_l. Turbulence dissipation also shows small differences among the cases except below 32 m (Figure 9b), which is basically a non-turbulent region. During the day, the solutions are more sensitive to c_l than at night (compare Figures 9a and 9c and Figures 9b and 9d). Furthermore, TKE is more sensitive to c_l at 3 m horizontal resolution (compare thick and thin dashed lines in Figures 9c and 9d) than at 1 m horizontal resolution (compare thick and thin dot-dashed lines in Figures 9c and 9d). This finding is significant because it implies that the control experiment, which has an even higher resolution, will be even less sensitive to the parameter c_l, or the subgrid lengthscale. This is an attribute that any LES model should posses. If increasing resolution does not result in a reduction of sensitivity to the free parameters of the SGS model used, the SGS model itself is perhaps grossly incorrect.

Acknowledgments. Funding for this research is provided by the Frontier Research Systems for Global Change through its sponsorship of the International Pacific Research Center (IPRC). The author wishes to thank the two anonymous reviewers for their comments and criticisms, which helped to improve the manuscript. The editorial assistance by Diane Henderson is greatly appreciated. This is SOEST publication 5564 and IPRC publication 89.

References

Denbo, D. W., and E. D. Skyllinsgtad, An ocean large-eddy simulation model with application to deep convection in the Greenland Sea, *J. Geophys. Res., 101*, 1095-1110, 1996.

Jerlov, N. G., *Optical Oceanography*, 194 pp., Elsevier, New York, 1968.

Langmuir, I., Surface motion of water induced by wind. *Science, 87*, 119-123, 1938.

Large, W. G., and P. R. Gent, Validation of vertical mixing in a equatorial ocean model using large eddy simulations and observations. *J. Phys. Oceanogr., 29*, 449-464, 1999.

Large, W. G., J. C. McWilliams, and S. Doney, Oceanic vertical mixing: a review and a model with a nonlocal boundary layer parameterization, *Rev. Geophys., 32*, 363-403, 1994.

McWilliams, J. C., P. P. Sullivan, and C.-H. Moeng, Langmuir turbulence in the ocean, *J. Fluid Mech., 334*, 1-30, 1997.

Moeng, C. H., A large-eddy-simulation model for the study of planetary boundary-layer turbulence, *J. Atmos. Sci., 41*, 2052-2062, 1984.

Paulson, C. A., and J. J. Simpson, Irradiance measurements in the upper ocean, *J. Phys. Oceanogr., 7*, 952-956, 1977.

Schumann, U., Subgrid length-scales for large-eddy simulation of stratified turbulence, *Theor. Comput. Fluid Dyn., 2*, 279-290, 1991.

Siegel, D. A., and A. Domaradzki, Large-eddy simulation of decaying stably stratified turbulence, *J. Phys. Oceanogr., 24*, 2353-2386, 1994.

Skyllingstad, E. D., and D. W. Denbo, An ocean large-eddy simulation of Langmuir circulations and convection in the surface mixed layer, *J. Geophys. Res., 100*, 8501-8522, 1995.

Skyllingstad, E. D., W. D. Smyth, J. N. Moum, and H. Wijesekera, Upper-ocean turbulence during a westerly wind burst: A comparison of large-eddy simulation results and microstructure measurements, *J. Phys. Oceanogr., 29*, 5-28, 1999.

Wang, D., W. G. Large, and J. C. McWilliams, Large-eddy simulation of the equatorial ocean boundary layer: Diurnal cycling, eddy viscosity, and horizontal rotation, *J. Geophys. Res., 101*, 3649-3662, 1996.

Wang, D., J. C. McWilliams, amd W. G. Large, Large-eddy simulation of the diurnal cycle of deep equatorial turbulence, *J. Phys. Oceanogr., 28*, 129-148, 1998.

Weinstock, J., Vertical diffusion in a stably stratified fluid, *J. Atmos. Sci., 35*, 1022-1027, 1978.

Weinstock, J., Vertical diffusivity and overturning length in stably stratified turbulence, *J. Geophys. Res., 97*, 12653-12658, 1992.

D. Wang, IPRC-SOEST, University of Hawaii at Manoa, 2525 Correa Road, Honolulu, Hawaii 96822. (email: wangd@soest.hawaii.edu)

(Received November 30, 2000; revised December 20, 2000; accepted December 28, 2000.)